Journal of Membrane Science 662 (2022) 121021

Contents lists available at ScienceDirect

Journal of Membrane Science

journal homepage: www.elsevier.com/locate/memsci

Large-area homoporous membranes (HOMEs) enabled by multiple annealing

Zhe Zhang, Can Chen, Shanshan Zhang, Xiangyue Ye, Jiemei Zhou, Yong Wang *

State Key Laboratory of Materials-Oriented Chemical Engineering, College of Chemical Engineering, Nanjing Tech University, Nanjing, 211816, Jiangsu, PR China

ARTICLE INFO

Keywords:
Homoporous membranes (HOMEs)
Block copolymers (BCPs)
Multiple annealing
Swelling-induced pore generation
High-precision separation

ABSTRACT

Homoporous membranes (HOMEs) featuring through pores with almost identical apertures, are highly desired for high-precision separations. It remains a major challenge to produce large-area HOMEs because the microstructure control and defect annihilation become increasingly difficult when membrane sizes are dramatically increased. Herein, we propose a multiple annealing strategy to fabricate large-area HOMEs. Polystyrene-*block*-poly(2-vinyl pyridine) (PS-*b*-P2VP) films are first coated on smooth and large substrates. Being annealed by chloroform vapor, perpendicularly aligned P2VP cylinders are formed within the films, and further converted into through pores via the mechanism of selective swelling-induced pore generation. It is shown that the conventional single-time annealing is inadequate to create the ordered through pores, because P2VP chains may have no sufficient time to locomote to the right position as required for the ideal hexagonally arranged ordering. By virtue of the multiple annealing, well-defined through pores can be generated after consecutive annealing for three times, as more P2VP chains aggregate into the ideally ordering position. The films are transferred and composited onto macroporous substrates, producing composite membranes with an effective area of up to ~100 cm^2. The resultant membranes exhibit excellent separation performances. Importantly, HOMEs can be fabricated on low-cost substrates via this strategy, highlighting their great promise in real-world applications of high-precision separations.

1. Introduction

Homoporous membranes (HOMEs), also known as isoporous membranes in the case the membrane pores are in the isotropic, cylindrical geometry [1], possess perpendicularly aligned through pores with nearly monodispersed apertures, and consequently endow membranes with extremely sharp selectivity and ultrafast permeability [2–4]. Having regularly structured nanoporosity, the permeability-selectivity relationship of HOMEs can be largely predicted, offering a promising design platform that is highly desired for advanced separation applications [5]. Therefore, HOMEs excel conventional polymeric membranes which tend to form tortuous porosities and scattered apertures. By virtue of such merits, HOMEs are capable of addressing the most demanding separation issues found in industry, i.e., the separation and purification of pharmaceuticals, proteins, noble metal nanoparticles and quantum dots [6–8]. Great effort has been made to prepare HOMEs, including polycarbonate membranes prepared by track etching [9], alumina membranes prepared by anodization of aluminum slices [10]. In addition, the micro/nanofabrication inspired by lithography as well as the vertical nanowire/tube arrays were also adopted to prepare HOMEs [11–14]. These fabrication techniques, however, inevitably suffer from inherent flaws of high cost, process complexity, intractable control over the pore ordering, shape, and size.

Block copolymers (BCPs) are hybrid macromolecules, in which incompatible homopolymer chains are strongly linked by covalent bonds [15,16]. Once activated by appropriate external fields, these covalently bonded polymer chains are prone to microphase separation, forming various periodical nanostructures of which the characteristic dimensions are typically in the range of 10–100 nm [17–19]. Therefore, BCPs offers an exciting opportunity to fabricate, under proper thermodynamics, separation membranes with perpendicularly aligned through pores [20,21]. It has been demonstrated that proper external stimulations allow the cylindrical phase to be perpendicularly aligned within the BCP matrix, and would be converted into cavities by chemical etching [22–26]. Nevertheless, the integrity of membrane frameworks as well as inherent surface chemistries are highly susceptible to such chemically irreversible and destructive approaches. In this vein, nondestructive alternatives for the fabrication of HOMEs are highly

* Corresponding author.
E-mail address: yongwang@njtech.edu.cn (Y. Wang).

https://doi.org/10.1016/j.memsci.2022.121021
Received 26 June 2022; Received in revised form 8 August 2022; Accepted 15 September 2022
Available online 19 September 2022

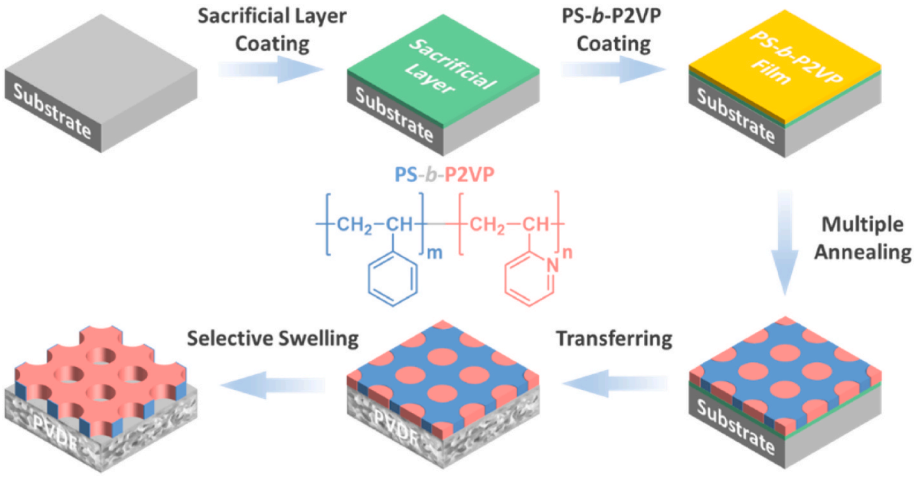

Scheme 1. Schematic depicting the preparation of HOMEs by a strategy of multiple annealing.

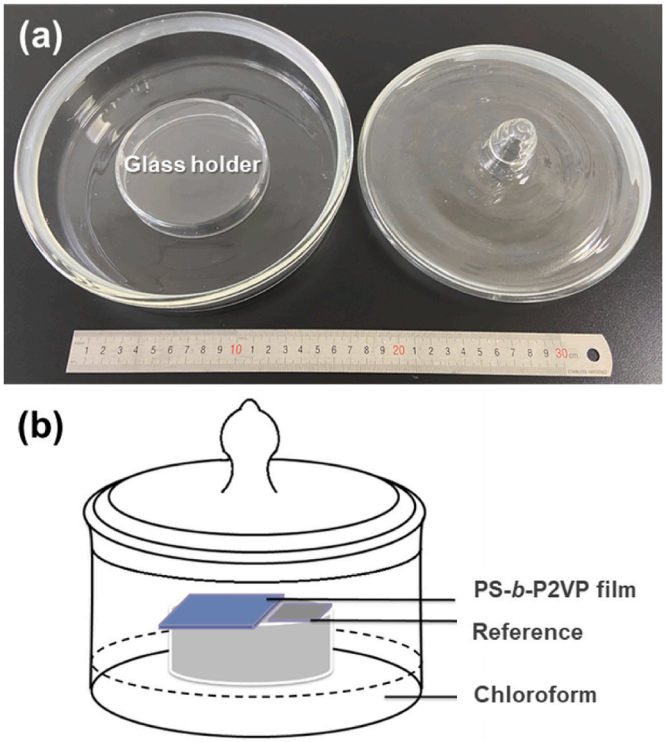

Fig. 1. Digital image (a) and schematic illustration (b) of the annealing chamber.

demanded. Orchestrating the microphase separation of BCPs and the macrophase separation of their films, a nondestructive strategy for the fabrication of asymmetrically structured HOMEs was developed [27–30]. Such asymmetrical and integral HOMEs composed of homoporous skin layers and sponge-like support layers were fabricated by the process of non-solvent induced phase separation (NIPS). Nonetheless, this method heavily relies on the large consumption of BCPs as the NIPS process produces the entire composition of the membranes including the separation layer and support layer.

We previously developed a nondestructive method for producing membranes with well-defined interconnected nanopores, which is named as selective swelling-induced pore generation [31–34]. The minority microdomains of amphiphilic BCPs are strongly swollen by the proper solvent, and subsequently collapsed and attached on the slightly swollen majority microdomains after being air-dried at room temperature. Taking polystyrene-*block*-poly(2-vinyl pyridine) (PS-*b*-P2VP) films as an example, this highly convenient method is also found to be applicable for the fabrication of HOMEs [35,36]. The PS-*b*-P2VP films are annealed in chloroform vapor, affording perpendicularly aligned P2VP cylinders embraced by the PS matrix. Subsequently, selective swelling is conducted to convert these cylinders into perpendicularly aligned through pores traversing the whole thickness of membranes. Notably, in this method the HOMEs are exclusively formed on macroporous substrates, and are serving as the selective layers with their thicknesses down to dozens of nanometers, thus consuming much less BCPs.

Up to date, HOMEs can be fabricated via a variety of strategies, however, these membranes are usually available as small-sized films with their areas typically less than 10 cm^2. This is mainly because the effective control over the membrane microstructures as well as the possible defect annihilation become increasingly difficult when the lateral sizes of the BCPs films are dramatically increased [4]. Although a few scalable methods seem to be promising [37–39], the large-scale manufacturing HOMEs still requires significant research efforts. Herein, we develop a strategy to fabricate large-area HOMEs via a multiple annealing process (Scheme 1). Dense and continuous PS-*b*-P2VP films were spin-coated onto silicon wafers with a diameter of 10 cm as well as glass plates with an edge length of 10 cm. Upon annealing in saturated chloroform vapor, PS-*b*-P2VP films featuring perpendicularly aligned P2VP cylinders surrounded by PS matrix were prepared. HOMEs were then obtained by selective swelling. We found that hexagonally arranged nanopores over the whole area of the films were nearly impossible to be created via single-time annealing as previously reported. With the annealing times progressively increased, much ordered through pores appeared, especially at the third time annealing. The annealed films were transferred onto macroporous substrate to produce composite membranes exhibiting excellent separation performances after the process of selective swelling-induced pore generation. Importantly, membranes prepared from the low-cost glass plates also exhibited homoporous pores and favourable separation performances, showing the great promise of the affordable preparation of large-area HOMEs for real-world applications.

2. Experimental section

2.1. Materials

PS-*b*-P2VP ($M_{n\ PS}$ = 290 kg mol^{-1}, $M_{n\ P2VP}$ = 72 kg mol^{-1}, polydispersity index (PDI) = 1.10) and hydroxy-terminated polystyrene (PS–OH, M_n = 6 kg mol^{-1}, PDI = 1.07) were obtained from Polymer

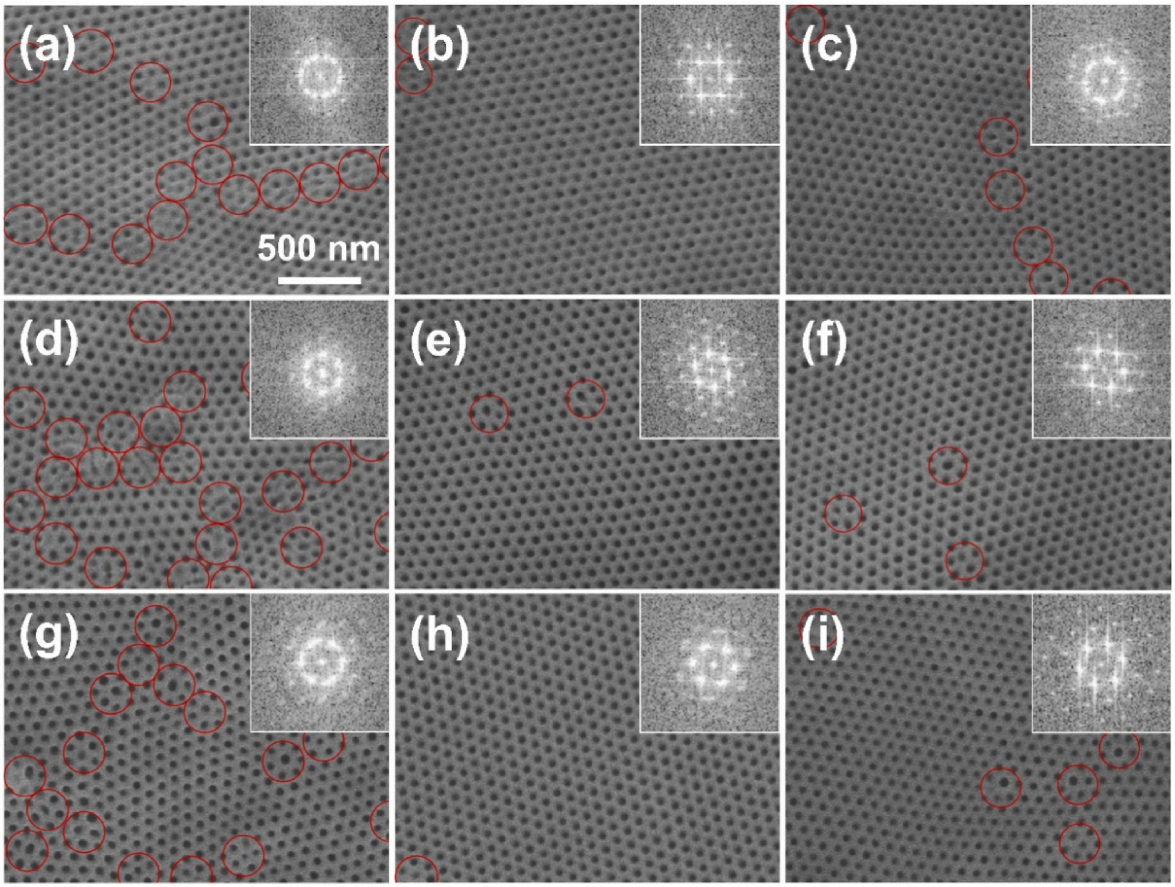

Fig. 2. SEM images of HOMEs on silicon wafers prepared from various annealing times. Surface morphologies of HOMEs prepared from the single-time annealing (a, d and g) with the PS-*b*-P2VP concentration of 1 wt% (a), 2 wt% (d) and 4 wt% (g). Surface morphologies of HOMEs prepared from the three-time annealing (b, e and h) with the PS-*b*-P2VP concentration of 1 wt% (b), 2 wt% (e) and 4 wt% (h). Surface morphologies of HOMEs prepared from the five-time annealing (c, f and i) with the PS-*b*-P2VP concentration of 1 wt% (c), 2 wt% (f) and 4 wt% (i). Scale bar in Fig. 1a applying to all images. Insets showing the corresponding FFT images. (For interpretation of the references to color in this figure legend, the reader is referred to the Web version of this article.)

Source Inc. Poly(sodium 4-styrenesulfonate) (PSS, M_w = 70 kg mol^{-1}, 20–30 wt% aqueous solution) was bought from Beijing Ouhe Technology Co., Ltd. Monodispersed gold particles (dispersed in water) with a diameter of 30 nm were obtained from BBI Solutions. Bovine serum albumin (BSA) as well as phosphate buffered saline (PBS) were purchased from MP Biomedicals, LLC. Other chemical reagents including chloroform, toluene, ethanol, and hydrofluoric acid (HF) were supplied by domestic suppliers. All reagents were in the analytical grade and used without further purification. To prepare PS-*b*-P2VP films, four-inch silicon wafers with a diameter of 10 cm (with a ~1-μm-thick sacrificial oxide layer) and square glass plates with an edge length of 10 cm were used as the smooth substrates. To prepare composite membranes, hydrophilic polyvinylidene fluoride membranes (PVDF, mean pore size of 0.22 μm, Merck Millipore) were used as the porous substrate. Deionized water was used throughout current work.

2.2. Membrane preparation

The membrane preparation contains five steps: (1) sacrificial layer coating, (2) PS-*b*-P2VP coating, (3) multiple annealing, (4) film compositing, and (5) selective swelling to produce homopores. During spin-coating and annealing, the temperature and relative humidity were maintained at 20 °C and 20%, respectively.

For substrate modification, silicon wafers were spin-coated with a thin layer of PS-OH, while glass plates were coated with a thin layer of PSS. PS-OH was first dissolved in toluene under sonication to produce a casting solution with PS-OH concentration of 0.1 wt%. Then, the solution was filtrated by a polytetrafluoroethylene filter (PTFE, 0.22 μm, Jinteng) to remove insoluble impurities possibly existing. The PS-OH solution was spin-coated on wafers at a speed of 1400 rpm and a duration of 30 s. After being heated under vacuum at 170 °C for 60 h, the wafers were soaked in toluene to remove unattached PS-OH. The as-received PSS solution was diluted with water to reduce the PSS concentration to a half. Then, the solution was spin-coated on glass plates with a speed of 2000 rpm and a duration of 30 s.

To prepare films, PS-*b*-P2VP was dissolved in chloroform to afford casting solutions with PS-*b*-P2VP concentrations of 1 wt%, 2 wt%, and 4 wt%, respectively. After that, the solutions were purified by the PTFE filter, and were spin-coated on silicon wafers or glass plates with a speed of 2000 rpm and a duration of 30 s.

In annealing process, chloroform was used as the annealing solvent. As shown in Fig. 1, 100 mL of chloroform was filled in a flat-bottom chamber with a diameter of 20 cm. Then, a glass holder was set in the bottom of the chamber, and the PS-*b*-P2VP films coated substrates were placed on its top surface. Given that the color of the film changed with the annealing proceeding, a ~200 nm-thick PS-*b*-P2VP film coated on silicon wafer as the reference to indicate the annealing process, was also placed in the chamber. Once the substrate was placed, the chamber was immediately sealed, allowing the PS-*b*-P2VP film to be completely exposed in the saturated chloroform vapor for annealing. When the color of the reference showed green, the annealing process was quenched by immediately uncovering the chamber to release the adsorbed chloroform inside the film. After that, the PS-*b*-P2VP films coated substrates were air-dried under room temperature. The above annealing process

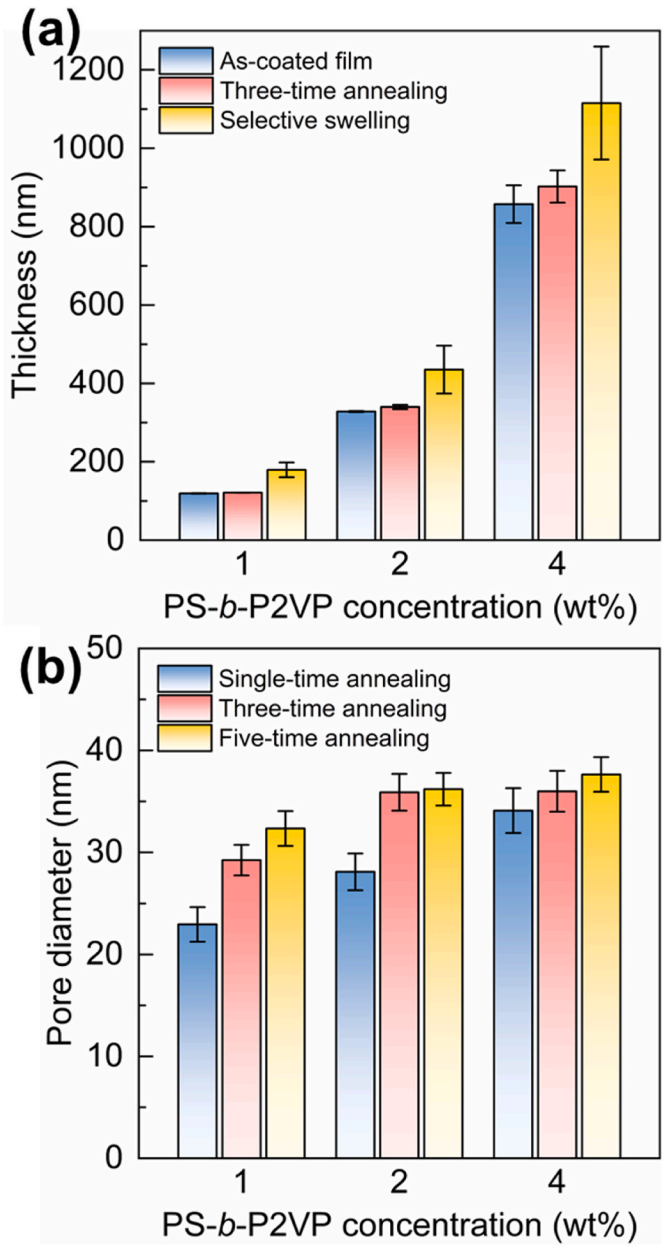

Fig. 3. Variation of thicknesses and pore diameters of the HOMEs on silicon wafers. Thickness (a) and pore diameter (b) of PS-*b*-P2VP films before and after the annealing and selective swelling prepared from different concentrations and various annealing times. (For interpretation of the references to color in this figure legend, the reader is referred to the Web version of this article.)

was repeated for different times, and the PS-*b*-P2VP films prepared from the first, the third and the fifth annealing were used for further studies.

After annealing, the PS-*b*-P2VP film coated substrates were immersed in the HF aqueous solution (5 wt%) or water to etch away the silicon oxide layer and PSS layer from the silicon wafers and glass plates, respectively. The PS-*b*-P2VP films were suspended in the etching liquid, and were transferred onto PVDF porous substrates. The PS-*b*-P2VP films transferred on PVDF were further air-dried at room temperature to enhance the adhesion between the film and the substrate. Subsequently, the obtained PS-*b*-P2VP/PVDF composite structures were immersed in ethanol at 65 °C for 8 h to implement the process of selective swelling-induced pore generation.

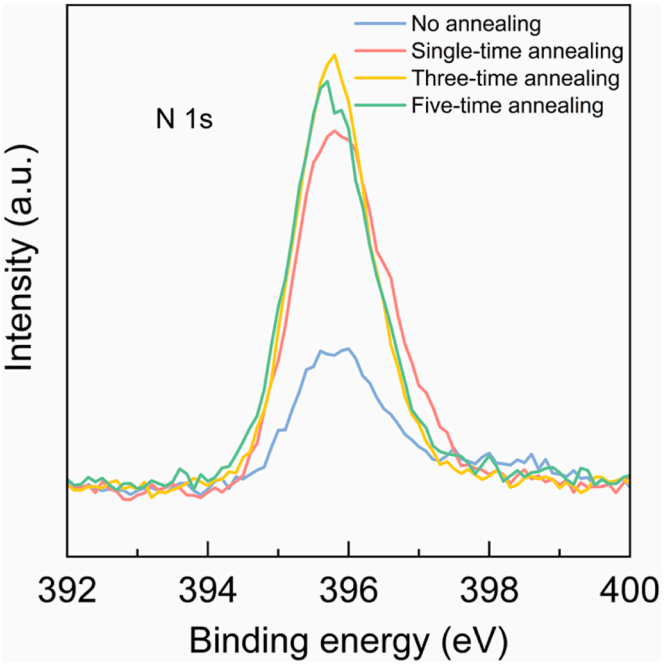

Fig. 4. XPS spectra of PS-*b*-P2VP HOMEs on silicon wafers prepared from various annealing times. (For interpretation of the references to color in this figure legend, the reader is referred to the Web version of this article.)

2.3. Characterizations

The surface and cross-sectional morphologies of PS-*b*-P2VP films and composite membranes were characterized by scanning electron microscopy (SEM, Hitachi S-4800) operating at a voltage of 3 kV. Before observation, samples were sputtering coated with a layer of gold under vacuum to reduce the discharging effect during SEM imaging. The thicknesses of PS-*b*-P2VP films before and after the selective swelling were measured by ellipsometry (Complete EASE M-2000U, J. A. Woollam) with a fixed incidence angle of 70°. X-ray photoelectron spectroscopy (XPS, K-Alpha, Thermo Fisher Scientific) was adopted to examine the nitrogen element on different membrane surfaces.

2.4. Separation performance test

The separation performances were evaluated using a dead-end filtration system (Amicon 8003, Merck Millipore) with a stirring speed of 600 rpm and a pressure of 0.4 bar. Prior to testing, the membranes were compacted under the same pressure for 10 min. The water permeance (L m^{-2} h^{-1} bar^{-1}) was obtained as follows:

$$Water\ Permeance = \Delta V / (A\ \Delta t\ \Delta p) \quad (1)$$

where ΔV (L) is the volume of the filtrate, A (m^2) is the active filtration area, Δt (h) is the filtration duration, and Δp (bar) is the pressure.

For rejection tests, aqueous solutions of BSA (0.5 g L^{-1}, prepared with PBS) and 30-nm gold particles (diluted 20-times with water) were used as the feed, respectively. Their concentrations were determined by the UV–vis spectrophotometry (NanoDrop 2000c, Thermo Fisher Scientific). The rejection rates (R, %) of BSA and gold particles were calculated as follows:

$$R = (1 - C_p / C_f) \times 100\% \quad (2)$$

where C_p and C_f are the concentrations of the permeated and the feed solutions, respectively.

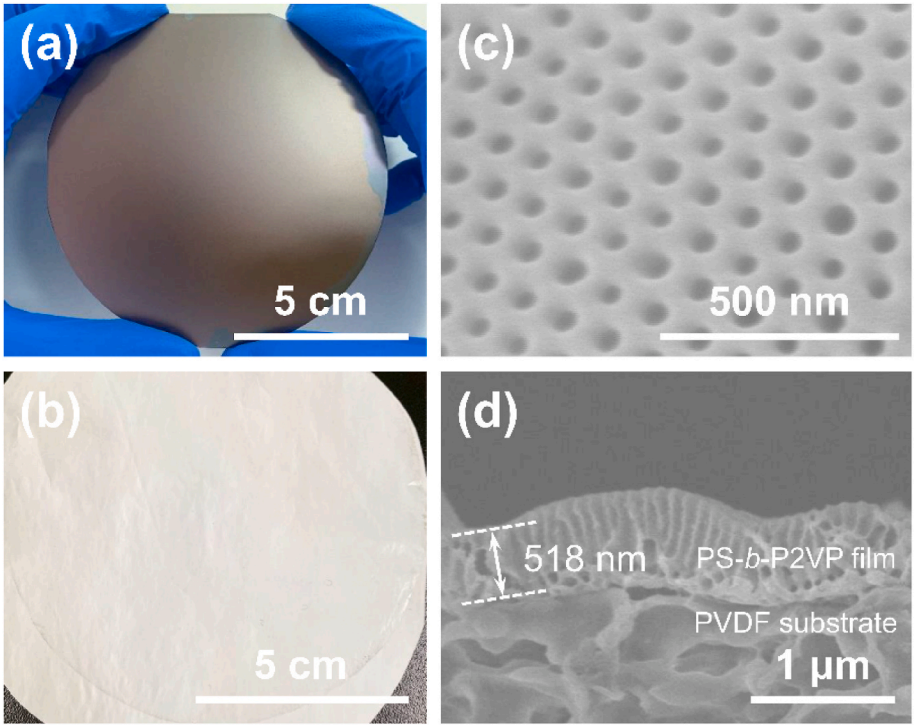

Fig. 5. The HOMEs prepared using silicon wafer as the smooth substrate with a PS-*b*-P2VP concentration of 2 wt% and three-time annealing. Digital images of (a) PS-*b*-P2VP film spin-coated on the silicon wafer and (b) the annealed and ethanol-treated PS-*b*-P2VP film composited on the PVDF substrate. SEM images of (c) surface and (d) cross section of the annealed and ethanol-treated PS-*b*-P2VP film composited on the PVDF substrate. (For interpretation of the references to color in this figure legend, the reader is referred to the Web version of this article.)

3. Results and discussion

3.1. Structures of HOMEs prepared on silicon wafers

The HOMEs were prepared by annealing the PS-*b*-P2VP films in chloroform vapor followed by selective swelling-induced pore generation [35,36]. Upon exposing the originally dense and nonporous PS-*b*-P2VP films to saturated chloroform vapor, chloroform would rapidly diffuse into PS and P2VP microdomains, due to the high affinity of chloroform to both PS and P2VP blocks. Thus, PS and P2VP blocks were highly solvated and gained significantly enhanced segmental mobility, thus facilitating the formation of P2VP cylinders anisotropically distributed in the PS matrix as a result of microphase separation. When annealing ended, the chamber was immediately opened and chloroform adsorbed in the PS-*b*-P2VP films was quickly evaporated from top surface to the interior, thus forming a vertical field of concentration gradient [40]. Driven by this field, P2VP cylinders were perpendicularly aligned in the PS matrix [41,42]. Such an aligned structure was fixed upon the complete evaporation of chloroform. With soaking the annealed films into hot ethanol, the P2VP chains would rapidly absorb ethanol so that the osmotic pressure was generated and accumulated in the P2VP cylinders. Driven by such osmotic pressure, the P2VP chains began to overflow onto the film surface from the P2VP cylinders. Meanwhile, the PS chains can be also plasticized with hot ethanol but to a moderate degree. The PS chains with enhanced mobility would be stretched along the direction normal to the film surface, while be compacted along the direction parallel to the film surface. Thus, this expanded the volume of the P2VP cylinders. When withdrawing the film from ethanol and drying at room temperature, the PS matrix was maintained at their stretched state due to the significantly reduced mobility of the PS at room temperature. However, after evaporation of ethanol, the P2VP chains shrank and collapsed onto the PS matrix, forming straight and through pores originating from the initially occupied P2VP cylinders. After selective swelling, the P2VP chains would line along the pore walls as well as on the film surface because they are covalently bonded to PS blocks.

Previously reported HOMEs were frequently received as small-sized films, i.e., less than 10 cm^2, to ensure the high degree of lateral order of through pores over the whole area of the films. In such a scenario, HOMEs can be produced via a single-time annealing in chloroform followed by selective swelling. However, to push HOMEs to real-world applications, large lateral sizes are essential. If the area of the PS-*b*-P2VP film drastically increases up to ~100 cm^2, which is about an order of magnitude higher than that of the previous small ones, the precise control over the highly ordered through pores becomes very challenging. In this work, we explore multiple annealing to prepare large-area PS-*b*-P2VP films with perpendicularly aligned P2VP cylinders, which is essential for the formation of HOMEs. The PS-*b*-P2VP films prepared from the concentration of 1 wt%, 2 wt%, and 4 wt% were first subjected to single-time annealing (Fig. 2a, d and g). Although the hexagonally arranged pores were successfully produced, a number of defects including non-perforated pores, enlarged and irregularly shaped pores (marked with red circles) also appeared. To reveal the pore regularity of these films, fast Fourier transformation (FFT) analysis was performed on SEM images (Insets of Fig. 2a, d and g). It was found that regularly aligned reflection spots were not obtained; instead, fuzzy and annular patterns appeared. This result is supportive of the presence of somewhat disordered pores in some local areas after single-time annealing. We then repeated the annealing process for another two times, that is, reaching the third annealing (Fig. 2b, e and h). Interestingly, the pores on the whole area of these films became much more ordered with clearly observed hexagonal characteristic and less defects (marked with red circles) compared with those of the single-time annealing. Moreover, the FFT patterns (Insets of Fig. 2b, e and h) demonstrated six-point patterns with highly aligned reflection spots, evidencing the hexagonally patterned pores existing on the whole PS-*b*-P2VP films after three-time annealing. Further repeating the process to reach the fifth annealing, highly ordered pores still can be seen on the whole PS-*b*-P2VP films (Fig. 2c, f and i). However, a few defects (marked with red circles) appeared, while the regularity of reflection spots in their FFT images became relatively weak (Insets of Fig. 2c, f and i). Note that the modification of the substrate with PS-OH is critical to the successful formation of the perpendicularly aligned P2VP cylinders and subsequently the homopores after selective swelling [36]. Based on the

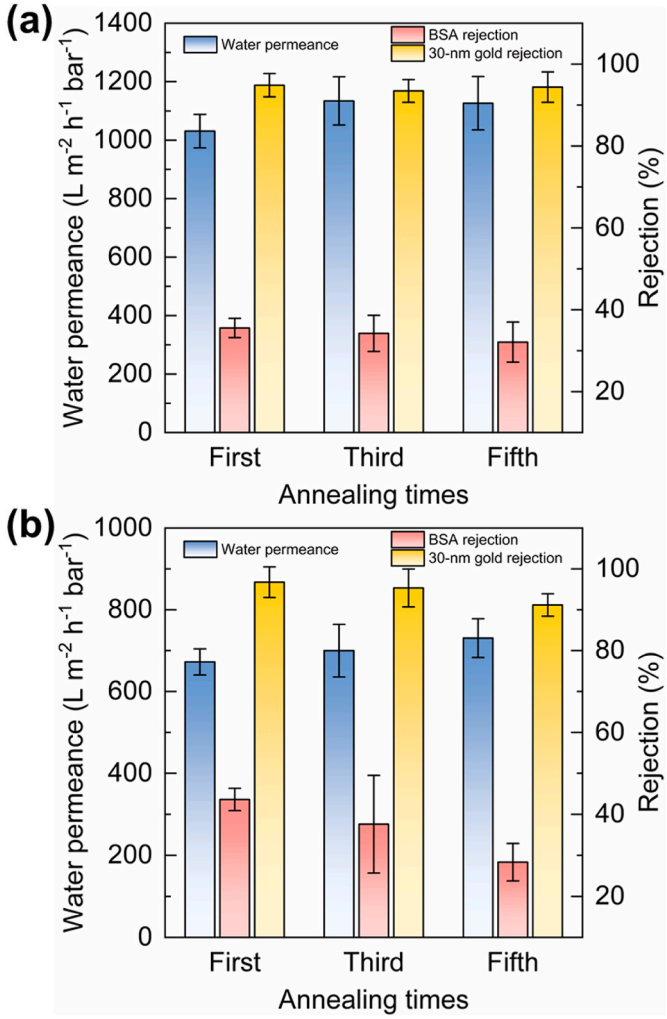

Fig. 6. Separation performances of the composite HOME membranes prepared from the PS-*b*-P2VP concentration of (a) 1 wt% and (b) 2 wt%.

above results, it is clear that hexagonally arranged uniform pores can be produced over large areas after performing the vapor annealing process for multiple times.

To further understand the effect of the multiple annealing process on the microstructures of the HOMEs, their thicknesses and pore diameters were measured. We used ellipsometry to examine the thicknesses of different films (Fig. 3a). The thicknesses of PS-*b*-P2VP films prepared from BCP solutions with the concentration of 1 wt%, 2 wt% and 4 wt% were 119 nm, 328 nm and 857 nm, respectively. The higher PS-*b*-P2VP concentrations resulted in larger thicknesses accordingly. After annealing for three times, the thicknesses of these films were increased to 121 nm, 340 nm and 902 nm, respectively. Thus, the multiple annealing process did not significantly change the thickness of films. This is mainly because chloroform merely influenced the mobility of PS and P2VP during the annealing process [35]. However, after selective swelling, the thicknesses of these films were sharply enlarged to 179 nm, 435 nm and 1115 nm, respectively. Such strong increases in thickness should be attributed to the volume expansion of the BCP film as a result of formation of pores after selective swelling. Besides, the film prepared from the concentration of 1 wt% has a larger relative change of the thickness (the thickness after selective swelling versus the original thickness) compared with those films prepared from higher concentrations. This can be attributed to the obvious expansion of the BCP framework more likely appeared in thin films, while such expansion would be restricted to some extent in thick films.

Furthermore, the different annealing times on the pore diameters were also investigated (Fig. 3b). With single-time annealing, the pore diameters of the HOMEs prepared from the concentration of 1 wt%, 2 wt % and 4 wt% were 23 nm, 29 nm and 32 nm, respectively. With three-time annealing, the pore diameters were enlarged to 28 nm, 36 nm and 36 nm, respectively. Further, with five-time annealing, the pore diameters were further enlarged to 34 nm, 36 nm and 38 nm, respectively. Interestingly, under the same annealing times, the pore diameter obtained from lower concentration is smaller than those obtained from higher concentrations. This might be ascribed to the stronger confinement effect of the substrate applied to thinner films, thus suppressing the swelling of P2VP cylinders to a larger degree. Consequently, smaller pores are produced after converting such thinner P2VP cylinders into through pores with the evaporation of ethanol. In addition, under the same concentration, the pores were enlarged with the increase of annealing times. On the basis of the solvent annealing mechanism, chloroform can easily penetrate into both PS and P2VP phases due to its high affinity to them both. Therefore, the mobility of PS and P2VP blocks was significantly enhanced for inducing the microphase separation, resulting in perpendicular alignment of P2VP cylinders. Given the very short duration of the annealing process that is usually less than 1 min, some P2VP chains may have no adequate time to locomote to the right position as required for the ideal hexagonally arranged ordering. This would lead to smaller and less ordering of the P2VP cylinders. Increasing the annealing times, more P2VP chains aggregate into the ideally ordering position, producing hexagonally arranged P2VP cylinders with the maximized diameter. The improved ordering and enlarged diameters of the P2VP cylinders with increasing annealing times were inherited by the corresponding through pores after selective swelling.

To gain more insights into the multiple annealing, we adopted XPS to detect the N element on the HOMEs prepared from the concentration of 1 wt% under different annealing times. As shown in Fig. 4, the peak intensity of N 1s was significantly intensified after annealing. More importantly, with the increase of the annealing times, the peak intensity of the N 1s was enhanced. As we have referred above, multiple annealing enabled P2VP cylinders inside BCP films nearly perfect alignment. Thus, these cylinders contained much quantity of the P2VP chains. After selective swelling and air-drying, massive P2VP chains were collapsed and firmly lined onto the PS matrix, forming the homoporous films. Because the N element merely exists in P2VP blocks, the intensified peak intensity indicated that more P2VP chains can be enriched on the surface of the homoporous films [32]. This result provides direct evidence to the applicability of the multiple annealing for creating much ordered homopores on large-area BCP films. In addition, three-time annealing appears to be optimal due to its strong peak intensity, which is consistent with the analysis from the SEM imaging. Notably, the above finding may suggest that potential kinetics control may exist during the multiple annealing process. It can be envisioned that large-area HOMEs with high ordering can be prepared using other BCPs after some proper optimizations guided by this multiple annealing strategy.

3.2. *Performances of HOMEs composited on macroporous substrates*

To evaluate the separation performances of the HOMEs, they were released from the smooth substrate by etching away the silicon oxide sacrificial layer with a diluted HF aqueous solution. Free-standing HOMEs layers were then transferred onto macroporous PVDF substrates, producing composite membranes with the homoporous PS-*b*-P2VP as the selective layer (Fig. 5a and b). SEM examination revealed that the surface of the composite membrane exhibits highly ordered, hexagonally arranged pores (Fig. 5c) while the cross section displays the perpendicularly aligned through pores with a thickness of 518 nm (Fig. 5d).

Fig. 6 displayed the water permeance, rejection to BSA and 30-nm gold particles of the composite HOME membranes prepared from the PS-*b*-P2VP concentration of 1 wt% and 2 wt% under different annealing

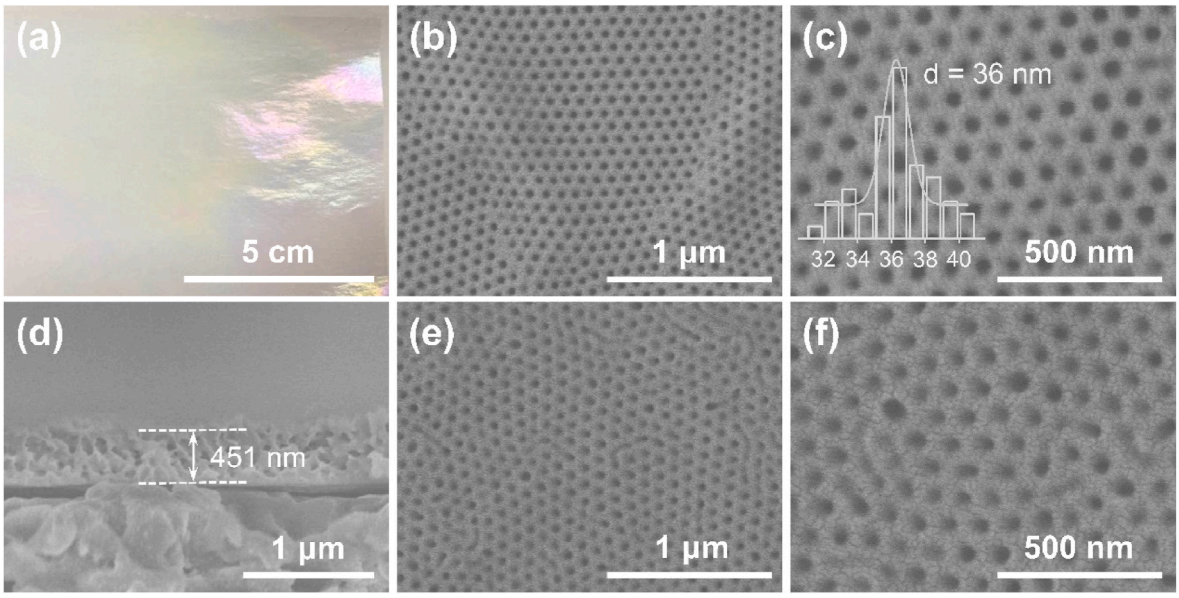

Fig. 7. HOMEs prepared using glass plate as the smooth substrate with a PS-*b*-P2VP concentration of 2 wt% and three-time annealing. (a) Digital image of the HOME composited on macroporous PVDF substrate. SEM images of the composite HOME membranes: (b) upper surface morphology in low magnification, (c) upper surface morphology in high magnification (Inset shows the pore diameter distribution), (d) cross-sectional morphology, (e) rear surface morphology in low magnification, (c) rear surface morphology in high magnification.

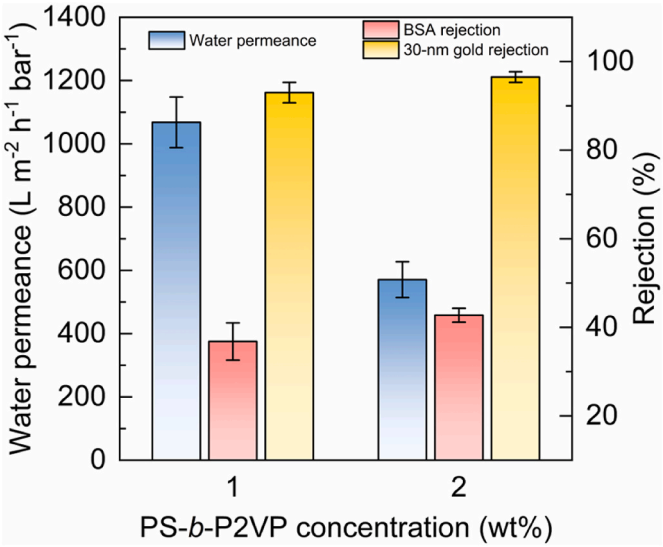

Fig. 8. Separation performances of composite HOME membranes prepared using glass plate as the substrate and three-time annealing.

times. In the case of the 1 wt% PS-*b*-P2VP, the composite HOME membranes exhibited analogous water permeance of 1031, 1134 and 1127 L m^{-2} h^{-1} bar^{-1}, respectively. Likewise, for 2 wt% concentration, composite HOME membranes exhibited similar tendency with the water permeance of 672, 700 and 731 L m^{-2} h^{-1} bar^{-1}, respectively. It is therefore concluded that, with the same PS-*b*-P2VP concentration, the water permeances were slightly increased by rising the annealing times. The perpendicularly aligned through pores as well as the hydrophilic P2VP chains lined on pore walls mainly account for the high water permeance. Note that the composite HOME membrane prepared from the concentration of 2 wt% has a slightly large pore size than that prepared from the concentration of 1 wt%, however, its water permeance is relatively low because of its much larger thickness. The sieving properties of the composite HOME membranes were revealed by the retention test using BSA and 30-nm gold particles as the probe. The composite HOME membranes prepared from the PS-*b*-P2VP concentration of 1 wt% exhibited the BSA rejection rates of 36%, 34% and 32%, respectively. For 30-nm gold particles, the rejection rates were 95%, 93% and 94%, respectively. Similarly, the composite HOME membranes prepared from the PS-*b*-P2VP concentration of 2 wt% demonstrated the BSA rejection rates of 44%, 38% and 28%, respectively. The rejection rates of 30-nm gold particles were 97%, 95% and 91%, respectively. In the case of same retention probe, both composite HOME membranes exhibited similar rejection characteristic, that is, the relatively low rejection rate to BSA (6.8 nm in diameter) and the high rejection rate to 30-nm gold particles. This is mainly because the multiple annealing processes did not substantially change the pore diameters, and the pore diameter of these membranes all falls in ~30 nm. Interestingly, the composite HOME membranes could reject BSA to a certain extent (~40% rejection rate), in spite of their pore sizes being larger than that of BSA. This finding could be ascribed to the relatively less porous bottom surface of membranes, and the BSA molecules being likely to form protein aggregates in water. Considering the uniform pore sizes of HOMEs prepare by this multiple annealing strategy, we expect that they would give good selectivity in the separation of mixtures of similarly sized solutes. In addition, optimal separation performances were obtained from the three-time annealing.

3.3. *Large-area HOMEs prepared from low-cost glass plates*

Above results proved that large-area HOMEs can be prepared using silicon wafers as the substrates, producing continuous and defect-free composite HOME membranes which exhibited good separation performances. However, from the view of practical applications, silicon wafers are too expensive on one hand and are not laterally large enough on the other to be used in the massive production of separation membranes. Therefore, the affordable preparation of large-area HOMEs still remains challenging. To this end, we proposed an easily accessible route to prepare large-area HOMEs on low-cost glass plates. In this case, the water-soluble polyelectrolyte, PSS, was pre-coated on the glass plates, forming an ultrathin sacrificial layer. The PS-*b*-P2VP HOMEs were prepared with a PS-*b*-P2VP concentration of 2 wt% and three-time annealing. The subsequent preparation procedures were the same to

the case of using silicon wafers as the substrates. After dissolving the PSS layer by water, free-standing HOMEs were conveniently transferred and composited onto the PVDF substrate (Fig. 7a). Highly ordered and hexagonally arranged nanopores with a diameter of 36 nm were observed on the whole upper surface (Fig. 7b and c), and the perpendicularly aligned through pores were also clearly observed throughout the 451 nm-thick cross section (Fig. 7d). Note that the nanopores on the rear surface seem to be slightly less ordered (Fig. 7e and f), mainly because the PSS chain coated on the glass may slightly hamper the mobility of P2VP blocks during the annealing process, disturbing the alignment of the pores to some extent [36]. Nevertheless, the pore diameter of the upper and the rear surfaces are almost the same.

We then performed the water permeation and the retention test on the composite HOME membranes prepared from three-time annealing using glass plates as substrates. As shown in Fig. 8, for the composite HOME membrane prepared from PS-*b*-P2VP concentration of 1 wt%, the water permeance was 1068 L m^{-2} h^{-1} bar^{-1}. The rejection rates of BSA and 30-nm gold particles were 37% and 93%, respectively. When the PS-*b*-P2VP concentration was 2 wt%, the water permeance was 571 L m^{-2} h^{-1} bar^{-1}. The rejection rates of BSA and 30-nm gold particles were 43% and 97%, respectively. These separation performances obtained here are close to those by using silicon wafer as the dense substrate. The separation performance tests were operated in a bench-scale operation using the typical dead-end mode. However, it should be noted that for practical applications, the cross-flow mode would be more suitable to minimize concentration polarization and membrane fouling potentially occurring. Therefore, it is obvious that the preparation of large-area HOMEs on low-cost glass plates is feasible, which is highly desired for the massive production and real-world applications of HOMEs.

4. Conclusions

In conclusion, we reported a multiple annealing method to fabricate large-area homoporous membranes (HOMEs). PS-*b*-P2VP was spin-coated on smooth substrates, followed by annealing in chloroform vapor. Perpendicularly aligned P2VP cylinders were formed within the PS-*b*-P2VP matrix, which were further converted into through pores via the mechanism of selective swelling-induced pore generation. The conventional single-time annealing was unable to produce highly ordered through pores, while the multiple annealing lent itself to enhance the regularity of the through pores covering the whole area. The films obtained from three-time annealing were found to be optimal, which were further transferred and composited onto macroporous PVDF substrates, affording composite HOME membranes with an active area of up to ~100 cm^2. The resultant membranes exhibited fast water permeation as well as the high rejection properties. It is also demonstrated that HOMEs can be fabricated from low-cost glass plates, which is essential to the affordable production of large-area HOMEs toward real-world applications of high-precision separations.

CRediT authorship contribution statement

Zhe Zhang: Investigation, Data curation, Writing – original draft, Writing – review & editing. **Can Chen:** Investigation, Data curation. **Shanshan Zhang:** Investigation, Data curation. **Xiangyue Ye:** Formal analysis. **Jiemei Zhou:** Formal analysis. **Yong Wang:** Conceptualization, Supervision, Writing – review & editing, Funding acquisition.

Declaration of competing interest

The authors declare that they have no known competing financial interests or personal relationships that could have appeared to influence the work reported in this paper.

Data availability

Data will be made available on request.

Acknowledgements

This work was funded by the National Science Fund for Distinguished Young Scholars (21825803).

References

[1] Y. Wang, Nondestructive creation of ordered nanopores by selective swelling of block copolymers: toward homoporous membranes, Acc. Chem. Res. 49 (2016) 1401–1408.
[2] J.R. Werber, C.O. Osuji, M. Elimelech, Materials for next-generation desalination and water purification membranes, Nat. Rev. Mater. 1 (2016), 16018.
[3] A. Lee, J.W. Elam, S.B. Darling, Membrane materials for water purification: design, development, and application, Environ. Sci.: Water Res. Technol. 2 (2016) 17–42.
[4] J. Zhou, Y. Wang, Selective swelling of block copolymers: an upscalable greener process to ultrafiltration membranes? Macromolecules 53 (2020) 5–17.
[5] R.Z. Waldman, F. Gao, W.A. Phillip, S.B. Darling, Maximizing selectivity: an analysis of isoporous membranes, J. Membr. Sci. 633 (2021), 119389.
[6] S.Y. Yang, I. Ryu, H.Y. Kim, J.K. Kim, S.K. Jang, T.P. Russell, Nanoporous membranes with ultrahigh selectivity and flux for the filtration of viruses, Adv. Mater. 18 (2006) 709–712.
[7] L. Guo, Y. Wang, M. Steinhart, Porous block copolymer separation membranes for 21st century sanitation and hygiene, Chem. Soc. Rev. 50 (2021) 6333–6348.
[8] Q. Lan, Z. Zhang, F. Xu, M. Wei, Y. Wang, Nanomeshes with sub-10 nm pores by glycerol-triggered 2D assembly in liquid phases for fast and selective membranes, Nano Lett. 21 (2021) 3302–3309.
[9] D.A. Bernards, T.A. Desai, Nanoscale porosity in polymer films: fabrication and therapeutic applications, Soft Matter 6 (2010) 1621–1631.
[10] H. Masuda, K. Fukuda, Ordered metal nanohole arrays made by a two-step replication of honeycomb structures of anodic alumina, Science 268 (1995) 1466–1468.
[11] T. Thurn-Albrecht, J. Schotter, G.A. Kästle, N. Emley, T. Shibauchi, L. Krusin-Elbaum, K. Guarini, C.T. Black, M.T. Tuominen, T.P. Russell, Ultrahigh-density nanowire arrays grown in self-assembled diblock copolymer templates, Science 290 (2000) 2126–2129.
[12] J.I. Lee, S.H. Cho, S.-M. Park, J.K. Kim, J.K. Kim, J.-W. Yu, Y.C. Kim, T.P. Russell, Highly aligned ultrahigh density arrays of conducting polymer nanorods using block copolymer templates, Nano Lett. 8 (2008) 2315–2320.
[13] C. Tang, S.-m. Hur, B.C. Stahl, K. Sivanandan, M. Dimitriou, E. Pressly, G. H. Fredrickson, E.J. Kramer, C.J. Hawker, Thin film morphology of block copolymer blends with tunable supramolecular interactions for lithographic applications, Macromolecules 43 (2010) 2880–2889.
[14] T. Xu, N. Zhao, F. Ren, R. Hourani, M.T. Lee, J.Y. Shu, S. Mao, B.A. Helms, Subnanometer porous thin films by the co-assembly of nanotube subunits and block copolymers, ACS Nano 5 (2011) 1376–1384.
[15] F.S. Bates, G.H. Fredrickson, Block copolymer thermodynamics: theory and experiment, Annu. Rev. Phys. Chem. 41 (1990) 525–557.
[16] I.W. Hamley, The Physics of Block Copolymers, Oxford University Press, USA, 1999.
[17] F.S. Bates, Polymer-polymer phase sehavior, Science 251 (1991) 898–905.
[18] S.B. Darling, Directing the self-assembly of block copolymers, Prog. Polym. Sci. 32 (2007) 1152–1204.
[19] Y. Mai, A. Eisenberg, Self-assembly of block copolymers, Chem. Soc. Rev. 41 (2012) 5969–5985.
[20] N. Hampu, J.R. Werber, W.Y. Chan, E.C. Feinberg, M.A. Hillmyer, Next-generation ultrafiltration membranes enabled by block polymers, ACS Nano 14 (2020) 16446–16471.
[21] J. Wang, M.M. Rahman, C. Abetz, V. Abetz, Bovine serum albumin selective integral asymmetric isoporous membrane, J. Membr. Sci. 604 (2020), 118074.
[22] A.S. Zalusky, R. Olayo-Valles, J.H. Wolf, M.A. Hillmyer, Ordered nanoporous polymers from polystyrene−polylactide block copolymers, J. Am. Chem. Soc. 124 (2002) 12761–12773.
[23] W.A. Phillip, J. Rzayev, M.A. Hillmyer, E.L. Cussler, Gas and water liquid transport through nanoporous block copolymer membranes, J. Membr. Sci. 286 (2006) 144–152.
[24] D.A. Olson, L. Chen, M.A. Hillmyer, Templating nanoporous polymers with ordered block copolymers, Chem. Mater. 20 (2008) 869–890.
[25] W.A. Phillip, B. O'Neill, M. Rodwogin, M.A. Hillmyer, E.L. Cussler, Self-assembled block copolymer thin films as water filtration membranes, ACS Appl. Mater. Interfaces 2 (2010) 847–853.
[26] A. Bertrand, M.A. Hillmyer, Nanoporous poly(lactide) by olefin metathesis degradation, J. Am. Chem. Soc. 135 (2013) 10918–10921.
[27] K.-V. Peinemann, V. Abetz, P.F.W. Simon, Asymmetric superstructure formed in a block copolymer via phase separation, Nat. Mater. 6 (2007) 992–996.
[28] S.P. Nunes, R. Sougrat, B. Hooghan, D.H. Anjum, A.R. Behzad, L. Zhao, N. Pradeep, I. Pinnau, U. Vainio, K.-V. Peinemann, Ultraporous films with uniform nanochannels by block copolymer micelles assembly, Macromolecules 43 (2010) 8079–8085.

[29] S.P. Nunes, A.R. Behzad, B. Hooghan, R. Sougrat, M. Karunakaran, N. Pradeep, U. Vainio, K.-V. Peinemann, Switchable pH-responsive polymeric membranes prepared via block copolymer micelle assembly, ACS Nano 5 (2011) 3516–3522.
[30] S.P. Nunes, M. Karunakaran, N. Pradeep, A.R. Behzad, B. Hooghan, R. Sougrat, H. He, K.-V. Peinemann, From micelle supramolecular assemblies in selective solvents to isoporous membranes, Langmuir 27 (2011) 10184–10190.
[31] Y. Wang, F. Li, An Emerging pore-making strategy: confined swelling-induced pore generation in block copolymer materials, Adv. Mater. 23 (2011) 2134–2148.
[32] Z. Wang, X. Yao, Y. Wang, Swelling-induced mesoporous block copolymer membranes with intrinsically active surfaces for size-selective separation, J. Mater. Chem. 22 (2012) 20542–20548.
[33] X. Shi, X. Wang, Y. Wang, Y. Wang, Producing nanoporosities in block copolymers within 30 s by microwave-boosted selective swelling, Macromolecules 53 (2020) 3619–3626.
[34] Y. Wang, C. Zhang, J. Zhou, Y. Wang, Room-temperature swelling of block copolymers for nanoporous membranes with well-defined porosities, J. Membr. Sci. 608 (2020), 118186.
[35] J. Yin, X. Yao, J.-Y. Liou, W. Sun, Y.-S. Sun, Y. Wang, Membranes with highly ordered straight nanopores by selective swelling of fast perpendicularly aligned block copolymers, ACS Nano 7 (2013) 9961–9974.
[36] W. Sun, Z. Wang, X. Yao, L. Guo, X. Chen, Y. Wang, Surface-active isoporous membranes nondestructively derived from perpendicularly aligned block copolymers for size-selective separation, J. Membr. Sci. 466 (2014) 229–237.
[37] K. Sankhala, J. Koll, M. Radjabian, U.A. Handge, V. Abetz, A pathway to fabricate hollow fiber membranes with isoporous inner surface, Adv. Mater. Interfac. 4 (2017), 1600991.
[38] K. Sankhala, J. Koll, V. Abetz, Setting the stage for fabrication of self-assembled structures in compact geometries: inside-out isoporous hollow fiber membranes, ACS Macro Lett. 7 (2018) 840–845.
[39] J. Wang, Md M. Rahman, C. Abetz, V. Abetz, Tuning the size selectivity of isoporous membranes for protein fractionation via two scalable post treatment approaches, J. Membr. Sci. 614 (2020), 118535.
[40] S.H. Kim, M.J. Misner, T. Xu, M. Kimura, T.P. Russell, Highly oriented and ordered arrays from block copolymers via solvent evaporation, Adv. Mater. 16 (2004) 226–231.
[41] W.A. Phillip, M.A. Hillmyer, E.L. Cussler, Cylinder orientation mechanism in block copolymer thin films upon solvent evaporation, Macromolecules 43 (2010) 7763–7770.
[42] K.A. Cavicchi, T.P. Russell, Solvent annealed thin films of asymmetric polyisoprene−polylactide diblock copolymers, Macromolecules 40 (2007) 1181–1186.